CHAM Case Study – CFD Modelling of Gas Dispersion from a Ruptured Supercritical CO_2 Pipeline

1. INTRODUCTION

This demonstration calculation concerns modelling the release and consequent gas dispersion into the atmosphere from a ruptured injection line conveying supercritical CO_2. The primary objective is to predict endpoint distances of the released gas at specified concentration levels. The study has been performed on behalf of Occidental Oil & Gas Corporation, Houston, Texas.

2. PROBLEM SPECIFICATION

The pipeline conditions are specified in Table 1, and as may be ascertained from Figure 1 the CO_2 exists as a supercritical fluid because the temperature (305K) and pressure (158.5 bar gauge) exceed their critical-point values of 304.1K and 73bar, respectively.

SCENARIO	DESCRIPTION	MATERIAL COMP	PRODUCT TEMP (F)	PRESS (PSIG)
Ruptured Source CO_2 Injection Line	6-inch Pipeline	0.7% H_2S & 99.3% CO_2 (Density 49.146 lb/ft^3, Liq SG 0.787596)	90	2300

Table 1: *Pipeline Conditions*

It can be seen that the product also comprises a small amount of H_2S, and the requirement is to predict endpoint distances at 40,000ppm for CO_2, and at 100, 300, and 500ppm for H_2S under the following meteorological conditions: F Class stability, 1.5 mph wind speed (0.671m/s), and an ambient temperature of 70F (294.1K).

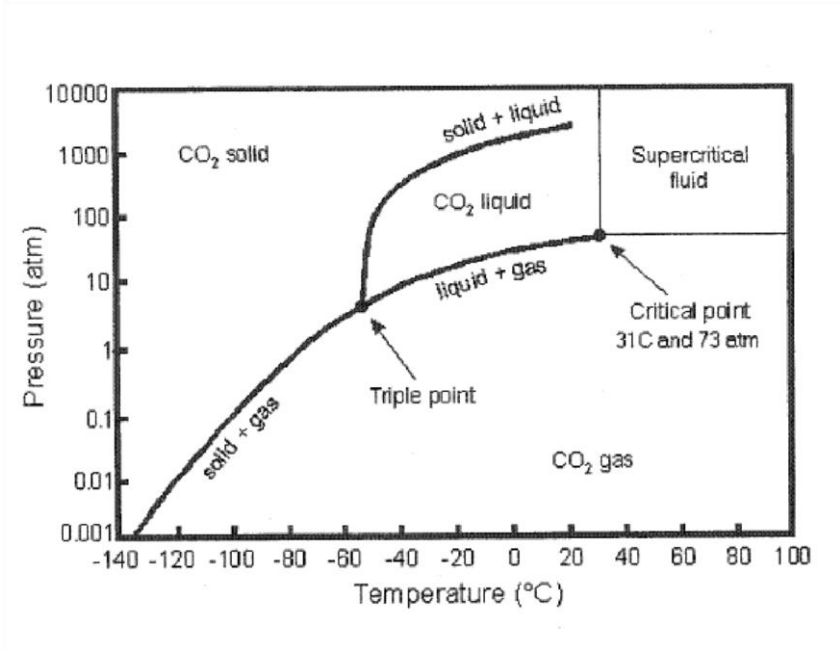

Figure 1: *CO_2 phase diagram*

2. COMPUTATIONAL STRATEGY

The requirement is to simulate using CFD modelling a steady, 3d turbulent, high-pressure, supercritical, two-component, heavy-gas release and its consequent dispersion into a wind environment with a stable atmosphere. For the purposes of this demonstration computation, a number of simplifying modelling assumptions have been made, as follows:

1. In the absence of any other information, a full-bore rupture of the horizontal pipeline has been modelled in open terrain. For computational economy, the solution domain for the gas-release scenario exploits flow symmetry by releasing the gas horizontally into the same direction as the wind.
2. The discharged gas is largely CO_2, and so it is modelled as pure CO_2 in terms of its physical properties. The field values of H_2S are deduced from the local mass fraction of discharged gas by reference to the mixture composition at source.
3. Pasquill Class F refers to stable stratification in the atmosphere with a prescribed linear profile for the ambient temperature, and a prescribed surface heat flux on the ground terrain. Since the Boussinesq approximation is not applicable in the present case, stable stratification complicates the treatment of buoyancy by means of a reduced hydrostatic pressure. Although it is straightforward to incorporate a suitably-modified buoyancy treatment into the dispersion model, for simplicity the demonstration will restrict itself to a neutral environment, namely Pasquill Class D.
4. The specified reference wind speed of 0.671m/s is presumed to prevail at a reference height of 10m. The surface roughness height is taken as 0.03m, which corresponds to open, flat terrain.
5. A two-stage computational approach is adopted whereby an analytical model is used to determine the discharge conditions at the rupture location by assuming steady choked flow.

These conditions are then used  provide inflow boundary conditions to a CFD model of the resulting gas dispersion.

6. It is not feasible to resolve the high-pressure discharge directly using CFD modelling within the context of flow in a much larger environment. This is due not only to its relatively small size, but also due to the computational difficulties in resolving the complicated underexpanded shock structure immediately downstream of the source. Although one might perform two separate CFD simulations, one for the near field discharge region so as provide inflow boundary conditions for a CFD dispersion analysis into the far field, it is much more expedient to employ an effective-source approach whereby the gas release is modelled from a plane downstream of the actual discharge position.
7. Strictly, real-gas effects should be taken into account, and especially in the analytical model for the inflow conditions at the discharge location. However, both for simplicity and demonstration purposes, ideal-gas behaviour is assumed in the field computations. The gasrelease inflow conditions are deduced by assuming ideal gas behaviour and by using the corresponding isentropic-flow relations. Nevertheless, in future studies a real-gas model can be used to compute the inflow conditions, such as for example by using either the RK, PR, VDW or the AN equation of states, as appropriate.
8. The effective-source approach referred to above can be modelled in a number of ways, but here a resolved-sonic approach is adopted whereby the discharge is representing as a sonic jet located some distance downstream of the actual discharge, but at atmospheric pressure with the actual discharge mass flow rate. This amounts to neglecting any entrainment between the actual source and the downstream sonic location. The effective discharge area is deduced from the pressure ratio by making some simple assumptions, and the location of the effective source is located roughly 6 pipe diameters downstream of the actual source, as determined by reference to experimental data on highly under-expanded jets. The INFORM facility of PHOENICS was used to implement both the analytical gas-discharge model and the effective-source model in the PHOENICS input file.
9. The possible formation of liquid or solid phases is ignored in the modelling.

3. MAIN FEATURES OF THE CFD MODEL

The CFD model of the dispersion process solves the steady-state, statistically-averaged conservation equations for mass, momentum, energy and discharge-gas continuity, together with transport equations for the turbulent kinetic energy k and its rate of dissipation ε. The turbulent Schmidt number of the discharge gas is taken as unity. The ground terrain is modelled using an empirical fully-rough log-law wall function, and the turbulence model includes buoyancy terms representing the influence of density gradients on turbulent mixing. The empirical coefficient controlling the buoyant creation/destruction of ε is taken as unity. For simplicity, the binary mixture of air and discharged gas employs uniform and equal specific heats for solution of the energy equation. The inflow conditions at the wind boundary (low-y) correspond to a fully-developed atmospheric boundary layer, and a fixed pressure condition is used at the side (high-x), top (high-z) and windflow exit (high-y) boundaries.

4. FLOW GEOMETRY, GRID SIZE & COMPUTATIONAL TIME

The CFD computation employs a non-uniform mesh comprising 162 cells in the transverse direction (x) covering 2km, 36 cells in the height direction (z) covering 100m, and 162 cells along the streamwise direction (y) covering 2km. The demonstration case aims only at showing the capabilities of PHOENICS in predicting the $C0_2$ dispersion. A larger solution domain has to be used if lower measurements of $C0_2$ and H_2S are to be predicted in the far field. The actual rupture source is located 30m downstream of the wind inflow boundary.

Although this is only a preliminary computation to demonstrate capability, care was taken to use a sufficient number of mesh cells for a reasonably adequate resolution of those regions with steep gradients of flow variables, such as for example, the discharge source and the ground-hugging dense gas layer. Budgetary constraints precluded the use of denser meshes coupled with optimal mesh distributions.

The steady-state computation typically required 5000 sweeps of the solution domain for complete convergence of the solution procedure. The solutions showed satisfactory overall conservation of mass, energy and CO_2 mass continuity. Convergence of the solution was demonstrated by the fact that the absolute whole-field sums of the residual errors in the mass continuity, energy and discharge-gas continuity equations were less than 1% of the total inflow values of these quantities. Further evidence of convergence was demonstrated by the fact that for every solved variable, the normalised maximum absolute value of the correction was less than 1%.

5. RESULTS

The CFD computation produces a large amount of detailed information including the threedimensional field distributions of the released chemical species in ppm by mass together with the velocity vector, pressure, temperature, density and turbulence parameters. Here, only a sample of the results is given through Figures 2 to 21. The main results of the simulations are summarised in Table 2 below, which shows the endpoint distances in each direction for various concentration levels in ppm by mass.

Gas	Coordinate	Endpoint distances (m)			
		40,000ppm	500ppm	300ppm	130ppm
CO_2	x	73m	-	-	-
	y	652m	-	-	-
	z	15m	-	-	-
H_2S	x	-	26m	65m	403m
	y	-	417m	607m	1664m
	z	-	11m	15m	23m

Table 2: *Predicted Endpoint distances from the actual source location*

Velocity, temperature and contaminants concentration fields

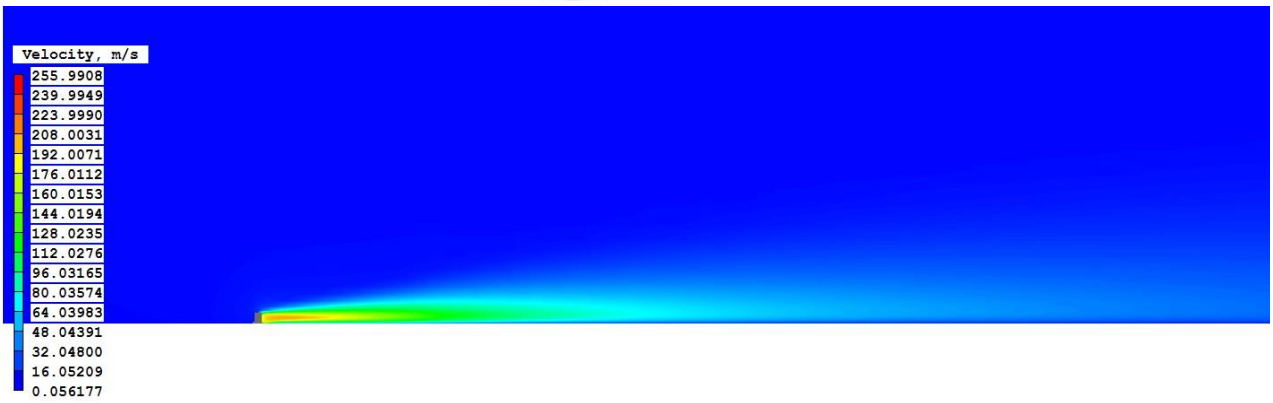

Figure 2: *Velocity Field- Side View*

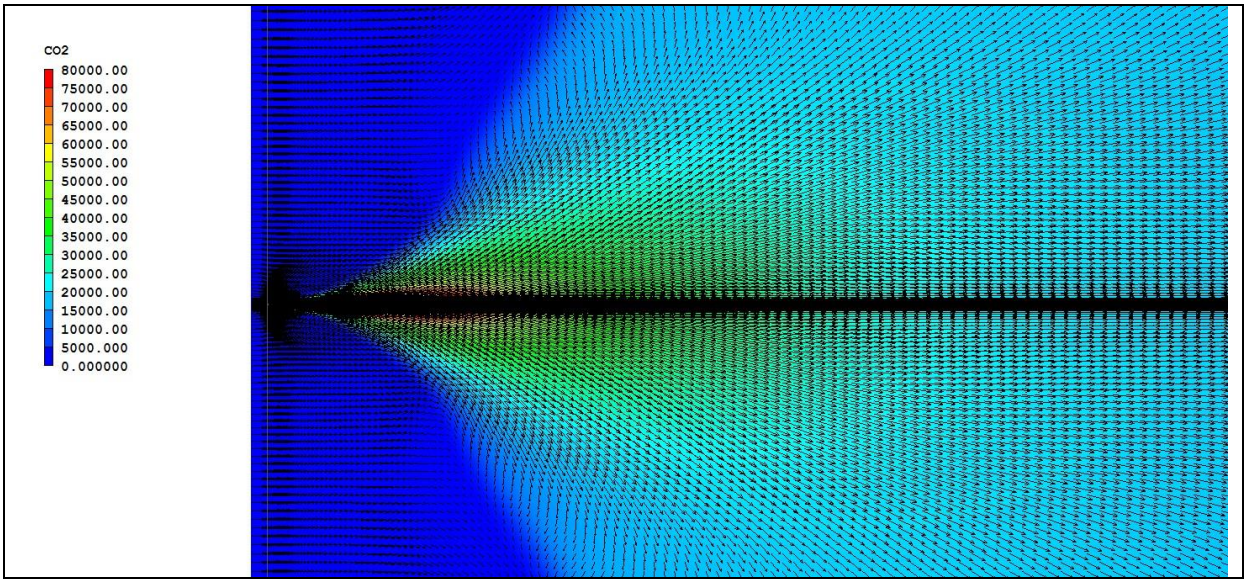

Figure 3: *Velocity Field- Particular and vector field coloured by CO_2 ppm*

Figure 4: *Temperature Field – Side View*

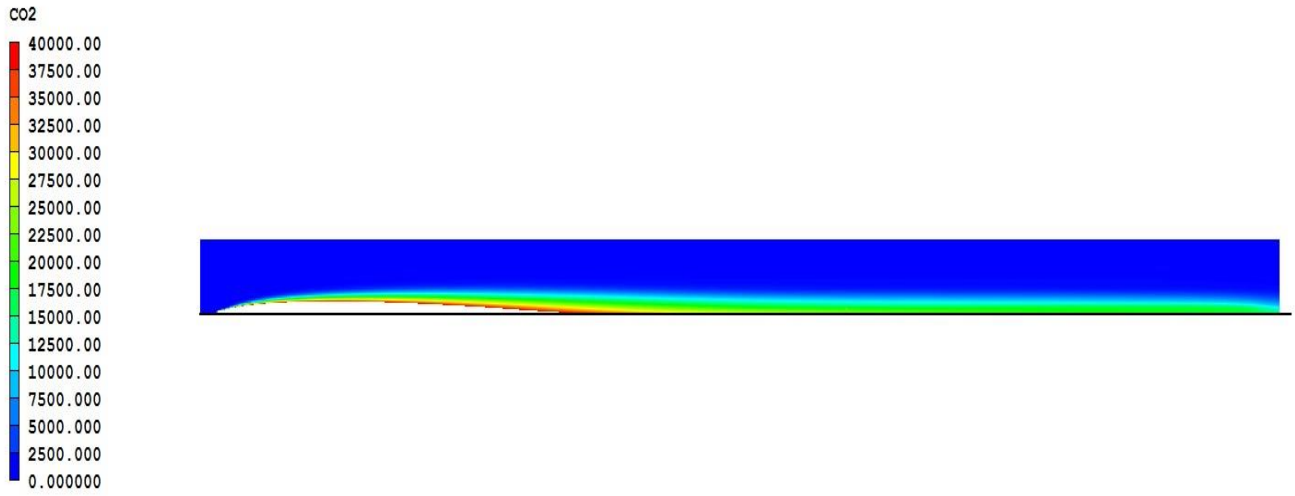

Figure 5: *$C0_2$ concentration in ppm –Side view. The maximum ppm showing is set at 40000*

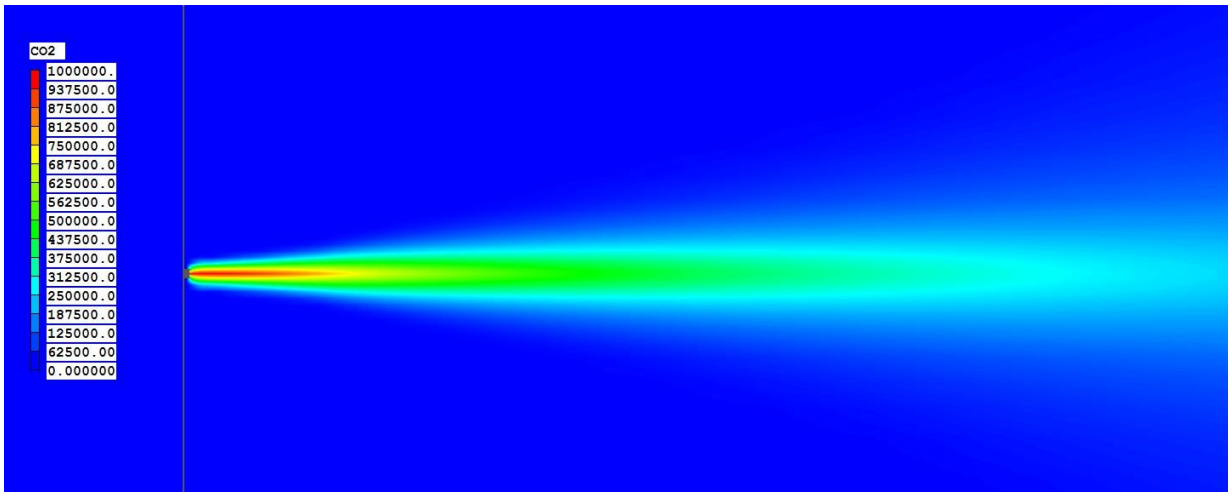

Figure 6: *$C0_2$ concentration in ppm –Top view (Zoomed)*

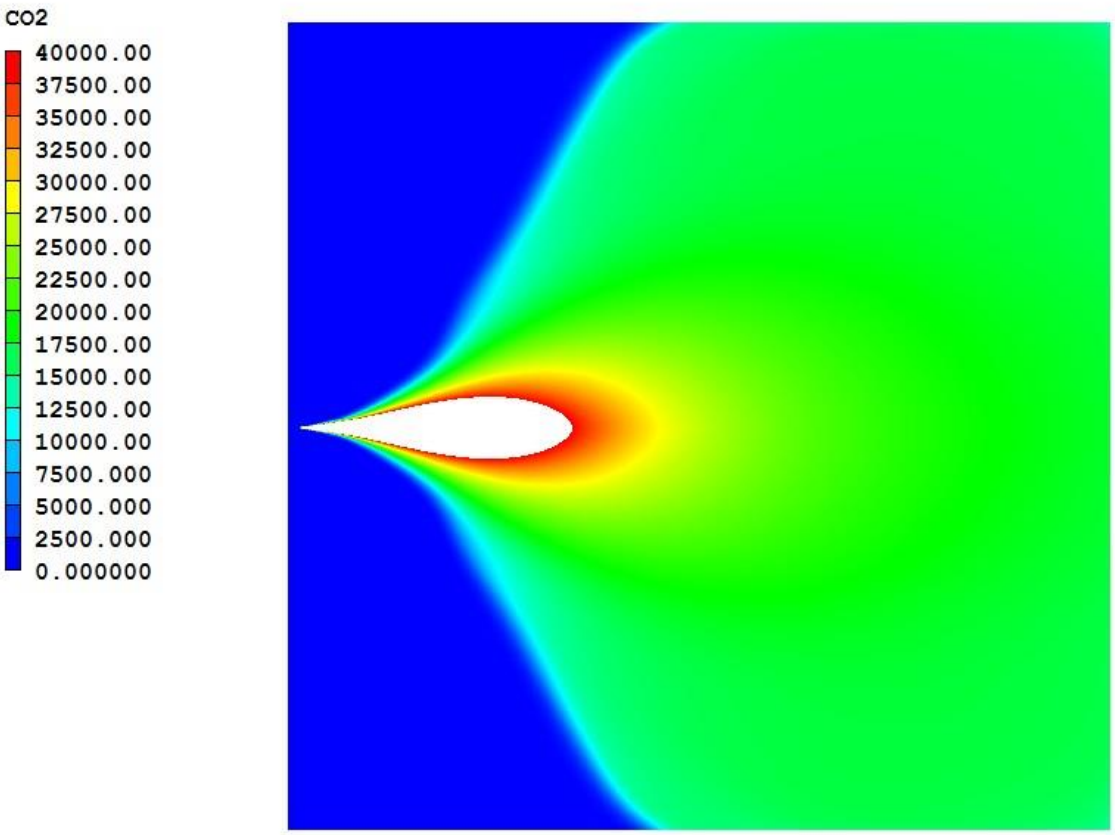

Figure 7: *CO_2 concentration in ppm –Top view. The maximum ppm showing is set at 40000*

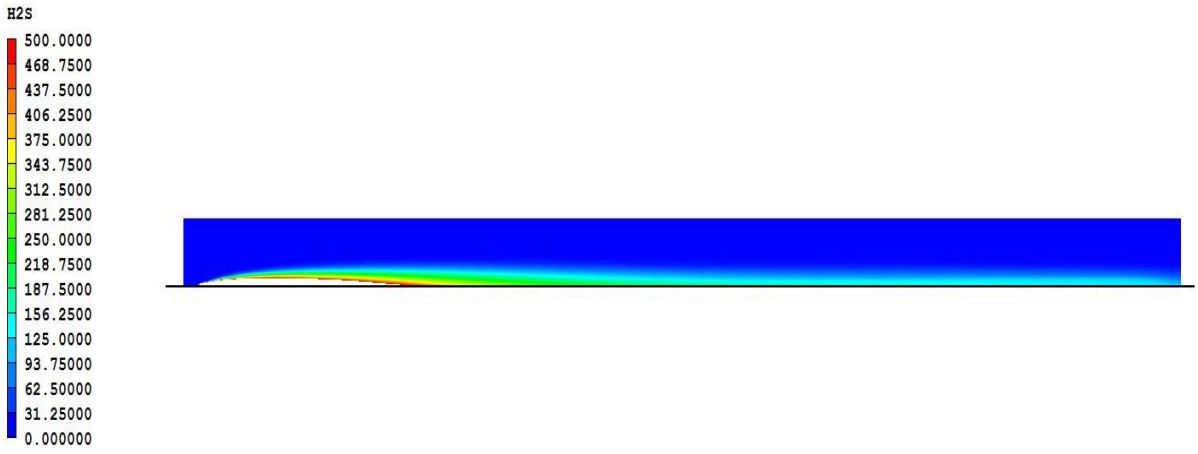

Figure 8: *H_2S concentration in ppm –Side view. The maximum ppm showing is set at 500*

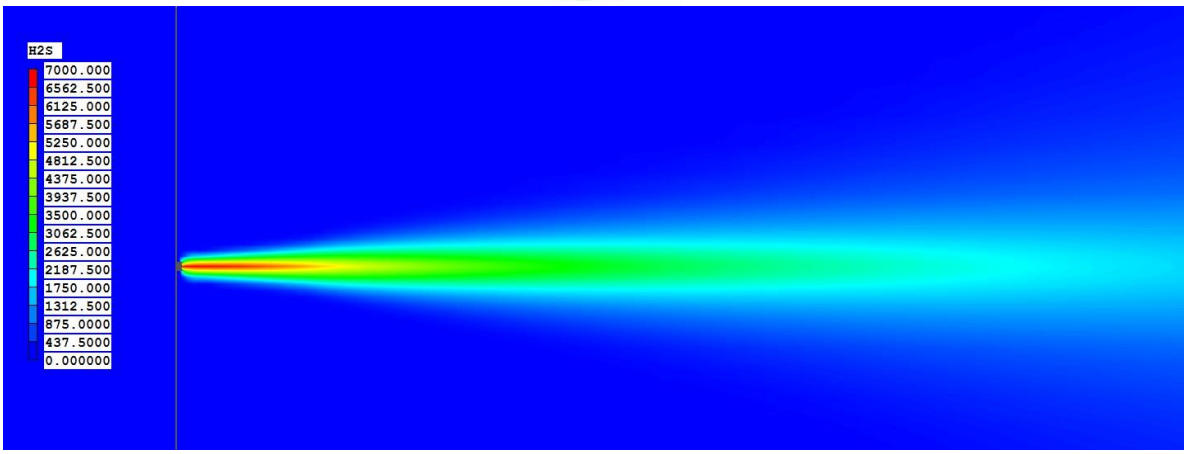

Figure 9: *H_2S concentration in ppm –Top view (Zoomed)*

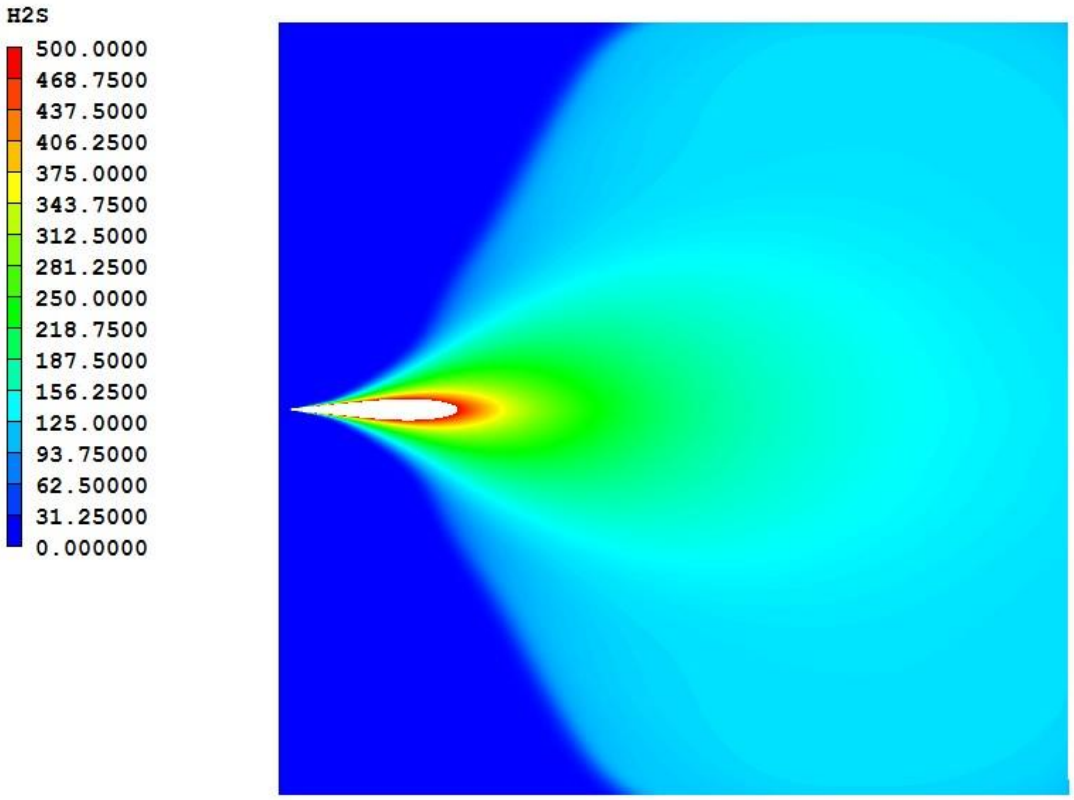

Figure 10: *H_2S concentration in ppm- Top view. The maximum ppm showing is set at 500ppm*

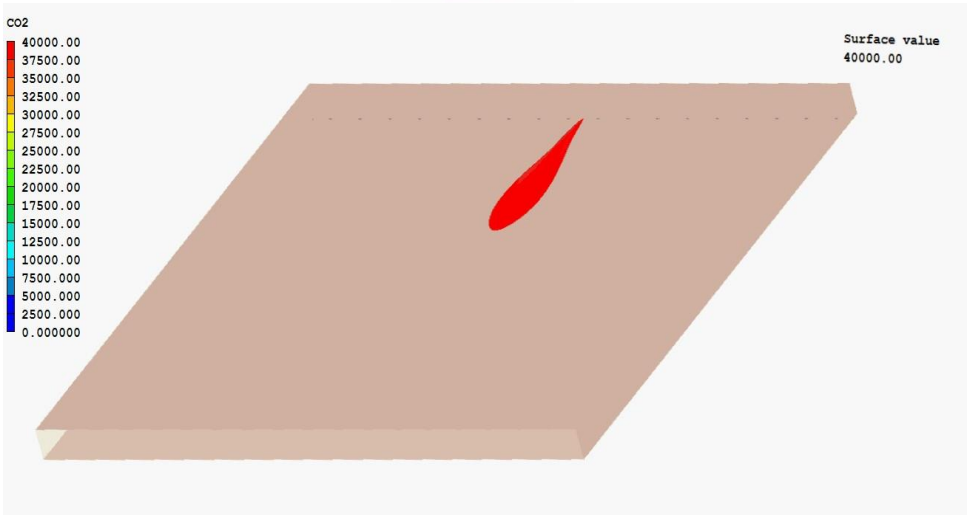

Figure 11: *Iso-surface of CO_2 concentration; 40000 ppm*

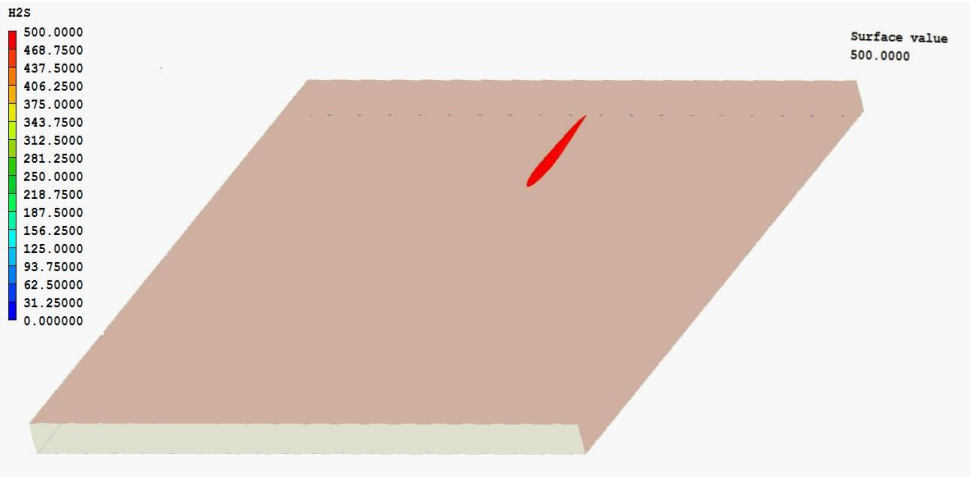

Figure 12: *Iso-surface of H_2S concentration at 500 ppm*

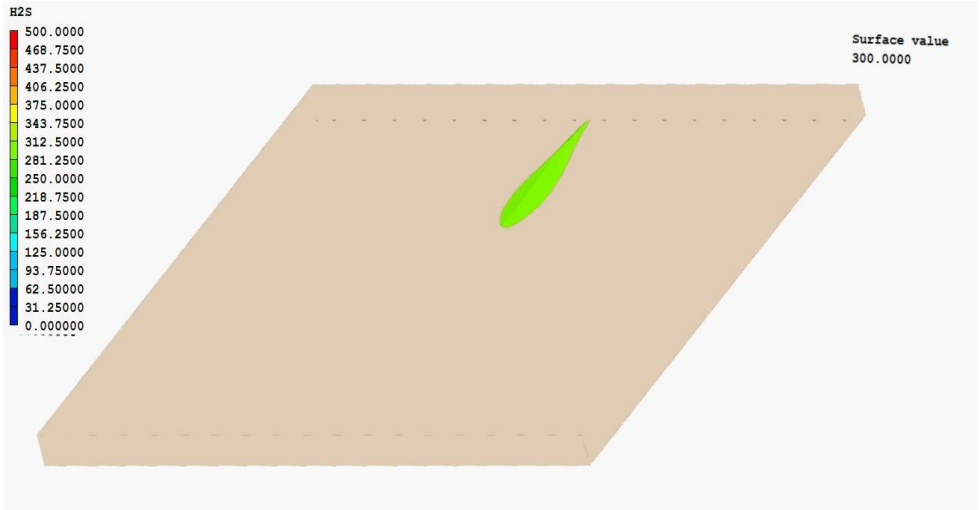

Figure 13: *Iso-surface of H_2S concentration at 300 ppm*

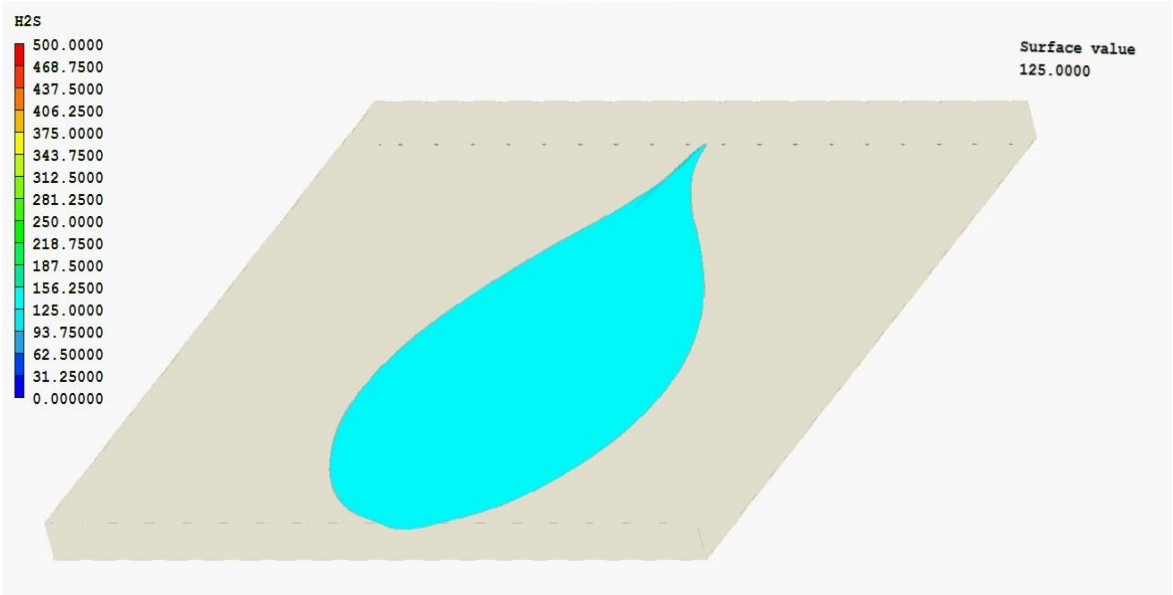

Figure 14: *Iso-surface of H_2S concentration at 125 ppm*

As expected the contaminants spreads mainly parallel to the ground. In order to show how the contaminants tend to embrace the ground a 1ppm CO_2 iso-surface is reported in Fig.16 (a + b).

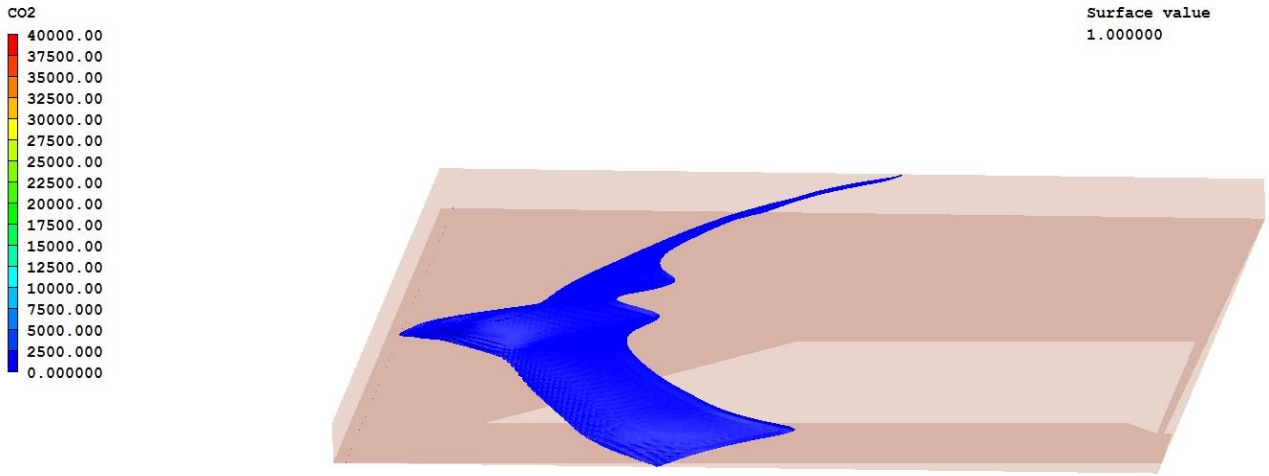

(a)

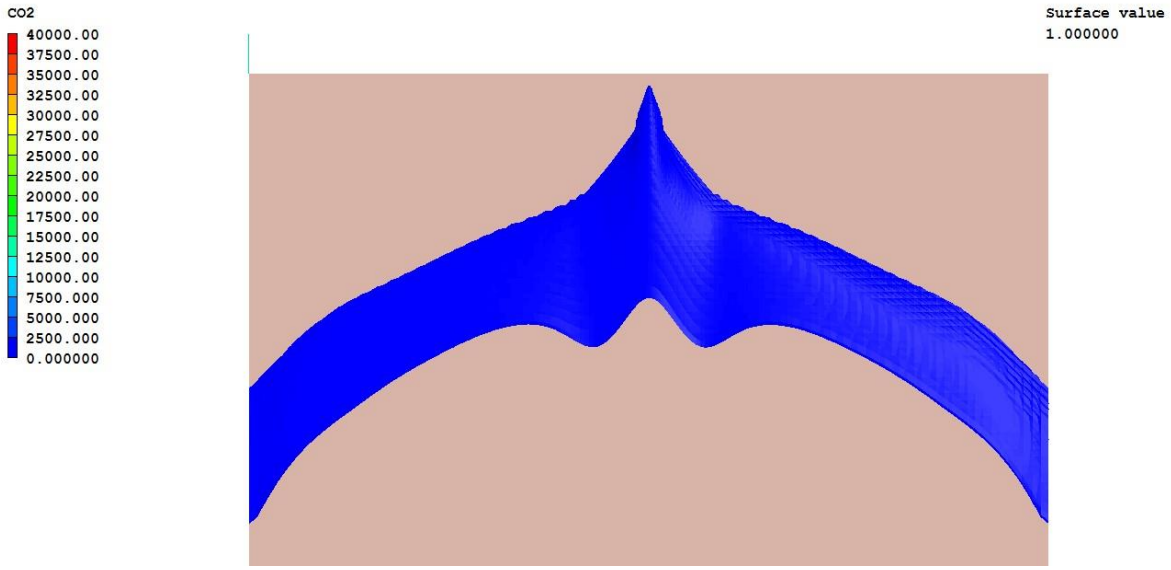

(b)

Figure 15: *Iso-surface of $C0_2$ concentration at 1 ppm*

<u>Stopping distances</u>

In this section the stopping distance for $C0_2$ is 40000 ppm, while for the H_2S they are 500, 300, and 130 ppm .

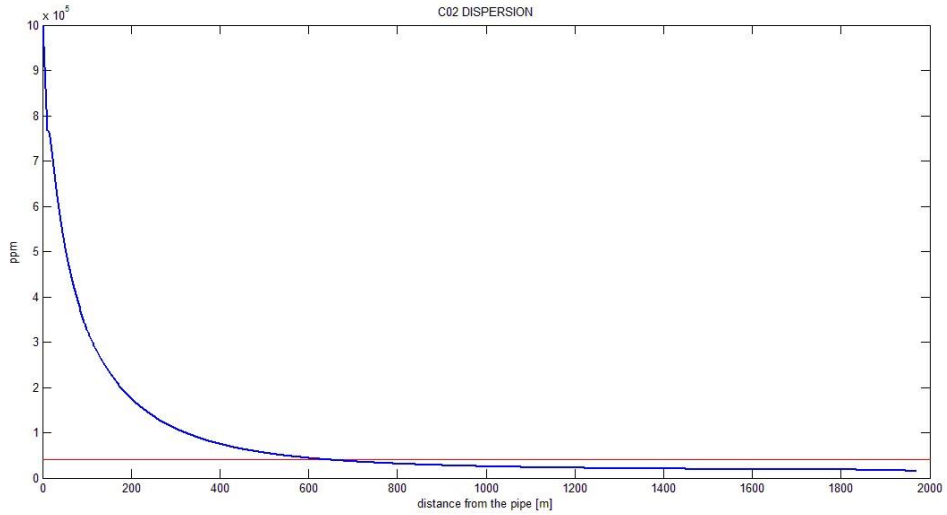

Figure 16: *CO2 dispersion in the y direction. In red the 40000 ppm concentration is highlighted*

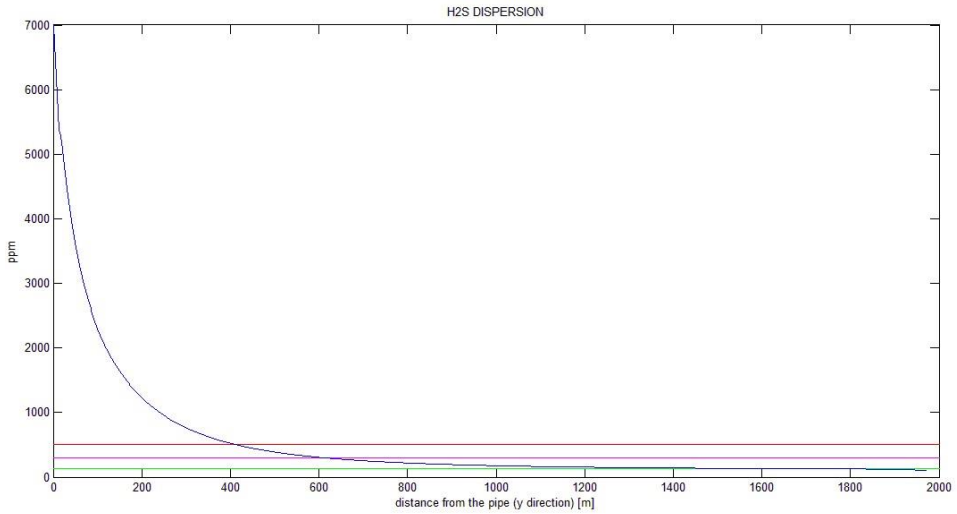

Figure 17: *H_2S dispersion in the y direction. The concentration at 500, 300 and 130 ppm are highlighted in red, magenta and green respectively*

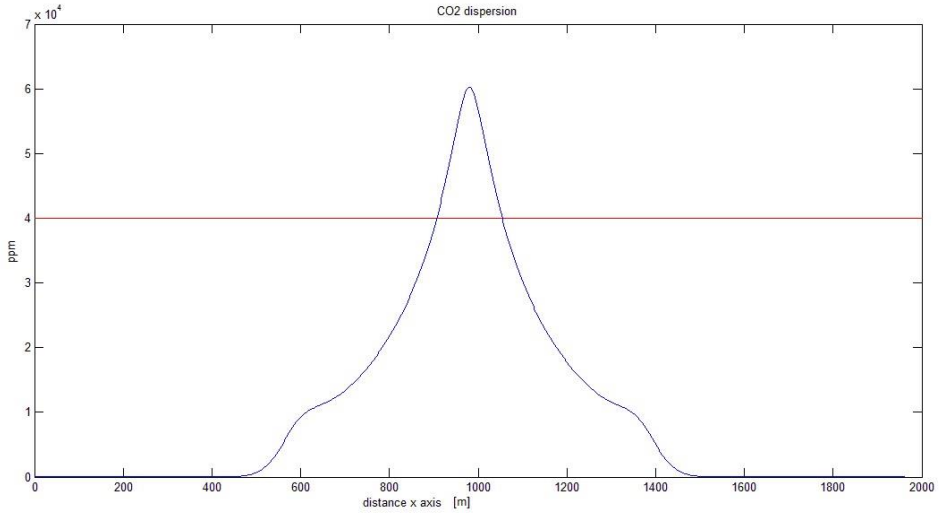

(a)

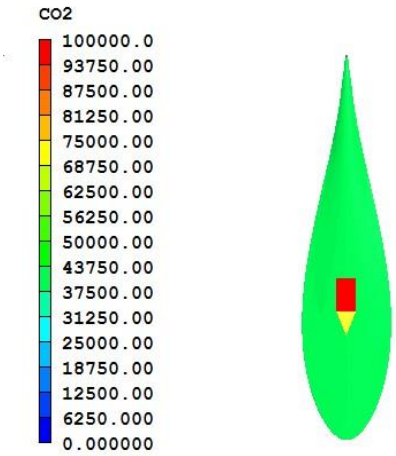

(b)

Figure 18: *a) CO2 dispersion in the x direction. The red line highlights the 40000 ppm concentration. These data are taken at 470m from the pipeline indicated by the probe position in b); b) CO_2 isosurface 40000ppm*

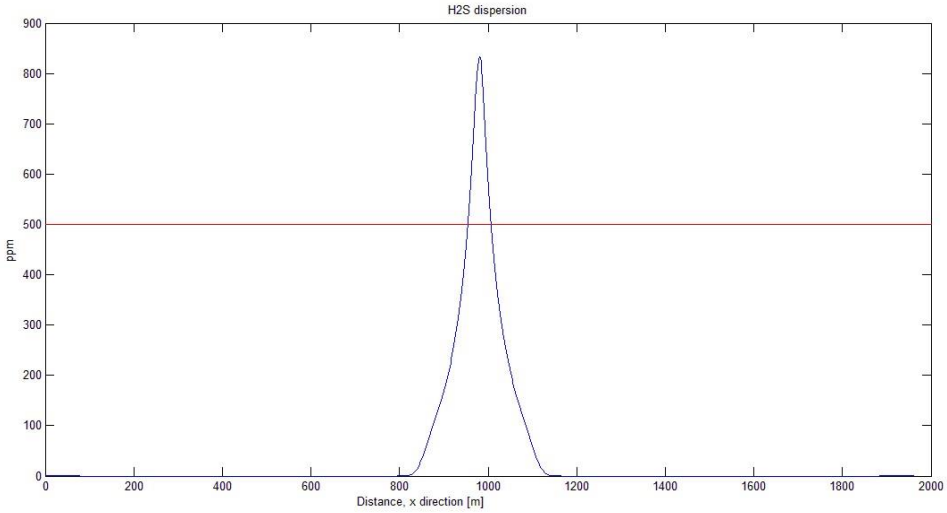

(a)

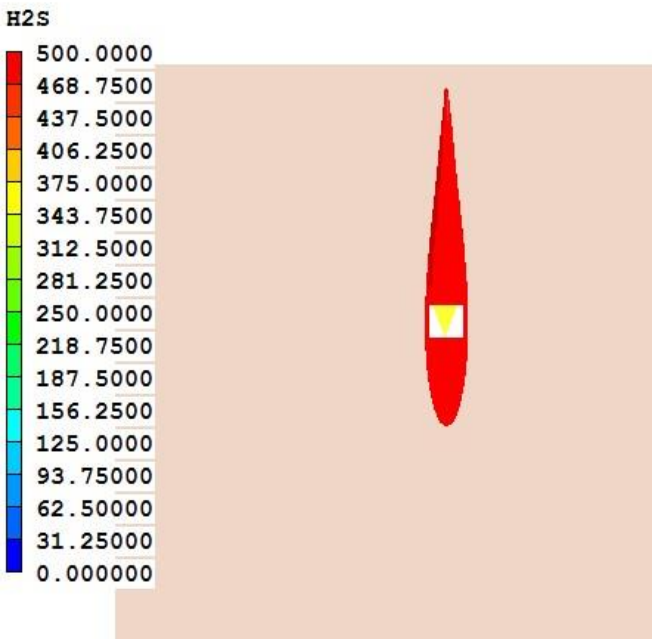

(b)

Figure 19: *a) H_2S dispersion in the x direction. The red line highlights the 500 ppm concentration. These data are taken at 270m from the pipeline indicated by the probe position in b); b) H_2S isosurface 500 ppm dispersion in the x direction.*

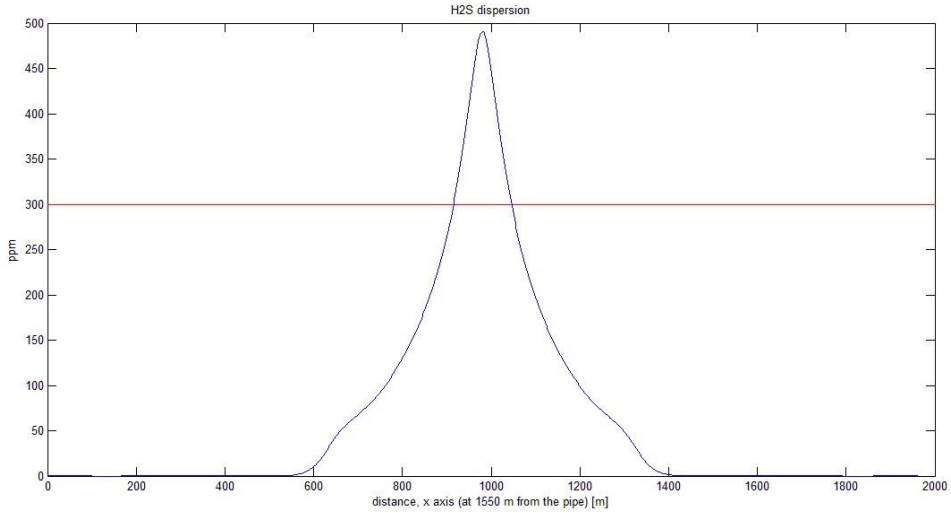

(a)

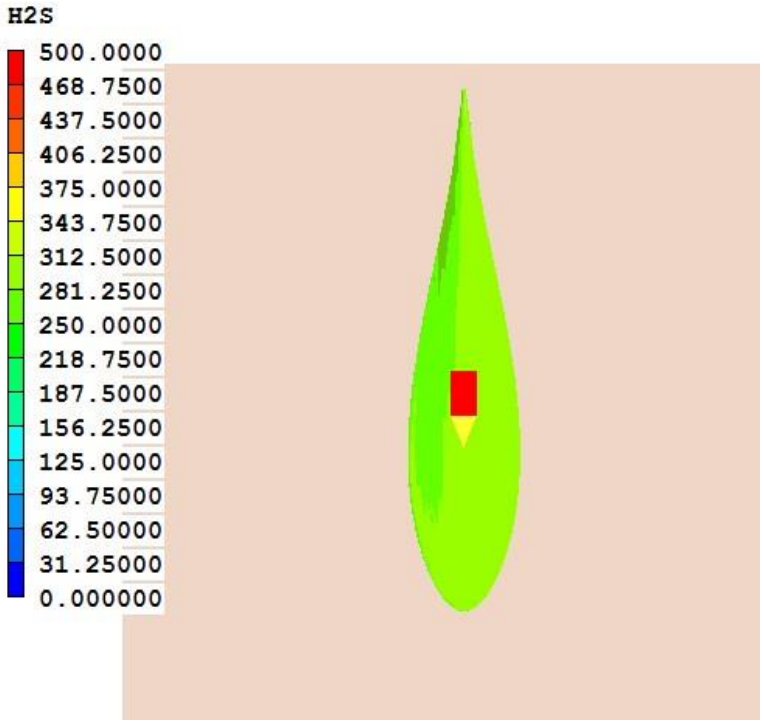

(b)

Figure 20: *a) H_2S dispersion in the x direction. The red line highlights the 300 ppm concentration. These data are taken at 420m from the pipeline indicated by the probe position in b); b) H_2S isosurface 300 ppm dispersion in the x direction.*

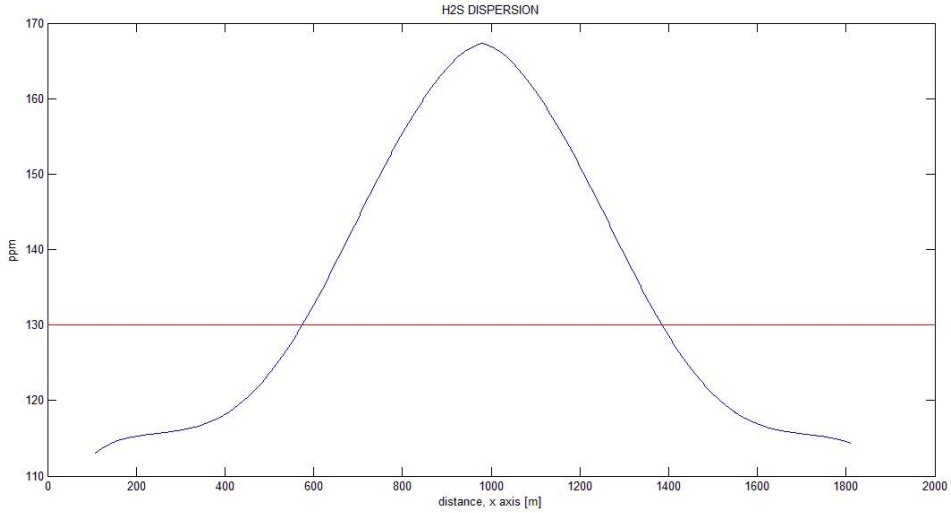

(a)

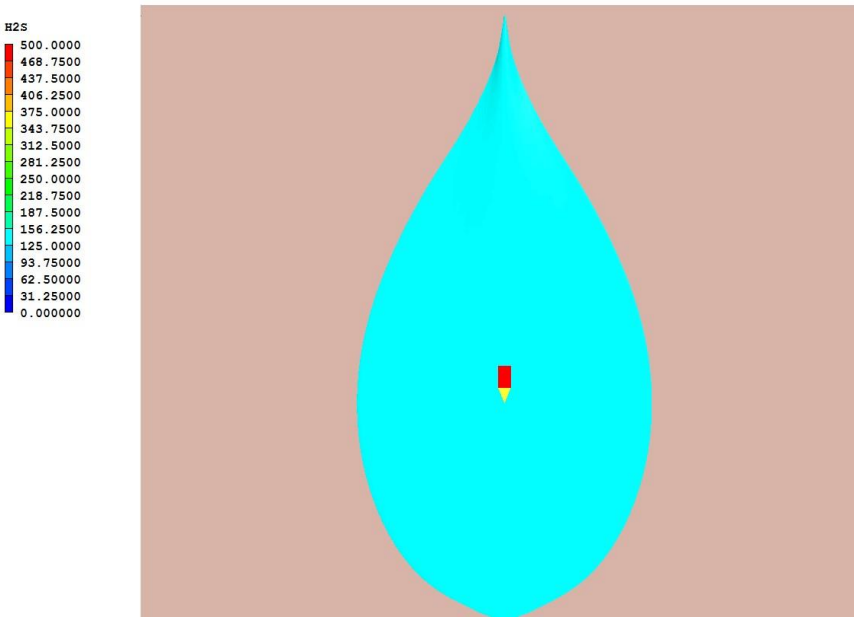

Figure 21: *a) H_2S dispersion in the x direction. The red line highlights the 130 ppm concentration. These data are taken at 1070m from the pipeline indicated by the probe position in b); b) H_2S isosurface 130 ppm dispersion in the x direction*

6. CONCLUSIONS

This case study demonstrates the capability of PHOENICS in analysing the dispersion of CO_2 from a rupture in a pipeline conveying supercritical CO_2. In order to predict efficiently the heavy-gas dispersion over a large environment a two-stage computational strategy has been employed which uses an analytical approach based on ideal-gas behaviour to determine the choked release conditions, and CFD modelling of the dispersion flow field together with an effective-source approach to circumvent the computational difficulties and expense involved in resolving the complex transonic system associated with the unexpanded jet in the near field.

The budgetary constraints of the present demonstration precluded any numerical studies aimed at optimising the domain size to accommodate H_2S levels as low as 100ppm, and studies aimed at optimising grid distributions and assessing the grid sensitivity of the solutions. For the same reason, no investigations were made of the influence upon the solutions of the turbulent Schmidt number, the dissipation-rate buoyancy coefficient, or the effects of accounting for real-gas behaviour. Likewise, there was insufficient time to perform a computation for a gas release into a stable environment, where one would expect the stably-stratified atmosphere to further inhibit CO_2 mixing and dilution. There is also scope to refine both the effective-source model, and the analytical model employed for determining the choked discharge conditions.

It should be mentioned that computational times could be reduced by using the PHOENICS solver in Parallel mode on a multi-processor pc.